

# Controlled Interfacial Assembly and Transfer of Brushlike Copolymer Films

Ronald V. Lerum and Harry Bermudez\*<sup>[a]</sup>

The self-assembly and compression of polybutadiene-*b*-poly(ethylene oxide) (PBd-PEO) at the air/water interface enables control over surface density, height, and film structure. Interfacial transfer was performed by a combination of Langmuir-Blodgett (LB) and Langmuir-Schaefer (LS) techniques, resulting in monolayer and bilayer films. Ellipsometry and wettability results were used to characterize the efficiency of transfer and to determine the properties of the resulting films, confirm-

ing a brushlike monolayer. Importantly, a high surface density is essential to obtain the desired film structure (i.e. a dense brush) and surface properties. The films were challenged by adsorption of fibrinogen, and the results are consistent with the notion of a PEO-enriched, and protein-repellant, bilayer surface. Such a bilayer film provides an opportunity for a tunable biomaterial interface to probe cell-surface interactions.

## Introduction

The creation of well-defined interfaces is important to many fields, ranging from industrial coatings to biomedical implants. Especially at the nanoscale, surface effects of chemistry and topography can dominate over the bulk material properties. Achieving the desired interfacial properties generally involves either small-molecule or macromolecular approaches; resulting in the alteration of pre-fabricated surfaces or the creation of new building blocks. Polymers in particular have been widely studied due to their roles as stabilizers and compatibilizers, where in this context chain configurations also become relevant.

Molecular and interfacial considerations are important regardless of the method used to create nanoscale polymer films: spin-coating,<sup>[1]</sup> layer-by-layer (LbL) deposition,<sup>[2,3]</sup> various grafting methods,<sup>[4,5]</sup> and interfacial transfer.<sup>[6–9]</sup> Spin-coating and LbL are rapid and inexpensive, and can achieve good 2D coverage. However, with the exception of simple (homo)polymers, both of the above methods do not allow control over the “grafting” or surface density. Grafting methods and interfacial transfer are able to provide increased control over surface density, but require more sophisticated chemistry and equipment. Finally, even if the films are extensively annealed, they may not necessarily reach equilibrium, and therefore sample history becomes a key contributor to film properties.

Herein, we focus on the creation of brushlike monolayer and bilayer block copolymer films by using the Langmuir-Blodgett<sup>[10]</sup> (LB) and Langmuir-Schaefer<sup>[11]</sup> (LS) methods. The LB and LS techniques have received attention to potentially create chemical sensors,<sup>[12]</sup> ranging from integrated circuits to biomimetic surfaces. A major strength of the LB and LS methods is the ability to externally impose molecular conformation and density of amphiphiles through compression at the air/water interface. Furthermore, the LB and LS methods can accommodate many different types of molecules: fatty acids, lipids, peptide-amphiphiles,<sup>[13]</sup> lipopolymers,<sup>[14,15]</sup> and block co-

polymers.<sup>[8,9,16–19]</sup> However, in spite of the attempts to create brushes, achieving strong chain overlap is actually quite rare. It is possibly for this reason that few studies to date have attempted the formation of a brushlike polymeric *bilayer* using combined LB/LS techniques.

Herein, through selection of interfacial conditions and the LB/LS technique, we have created brushlike block copolymer films of desired surface density, height, and structure. Furthermore, we have achieved efficient transfer of these films onto solid substrates. Our data support the notion that the bilayer films are hydrophilic in surface character, with hydrophobic segments of the polymer directed inwards towards a central region. Such bilayer film properties suggested nonfouling capabilities and potential as a biomimetic surface. Therefore, we tested and confirmed their resistance to protein adsorption.

## Results and Discussion

The interfacial behavior of polybutadiene-*b*-poly(ethylene oxide) (PBd-PEO) at room temperature can be represented by a surface pressure versus area ( $\Pi$ - $A$ ) isotherm (Figure 1). Several regions of polymer conformation can be defined from the isotherm and minima in the compressibility,  $k = -(1/A)(dA/d\Pi)$ .<sup>[20]</sup> In the so-called gaseous regime, the low surface density corresponds to a large area per molecule, and the film exhibits a low surface pressure. This small but finite surface pressure indicates that the copolymer remains at the interface, consistent with the known surface activity of PEO homopolymers.<sup>[21–24]</sup> With increasing density at the surface due to molec-

[a] Dr. R. V. Lerum, Prof. H. Bermudez  
Department of Polymer Science and Engineering  
University of Massachusetts, Amherst  
120 Governors Dr., Amherst, MA 01003 (USA)  
Fax: (+1) 413-585-8900  
E-mail: bermudez@polysci.umass.edu

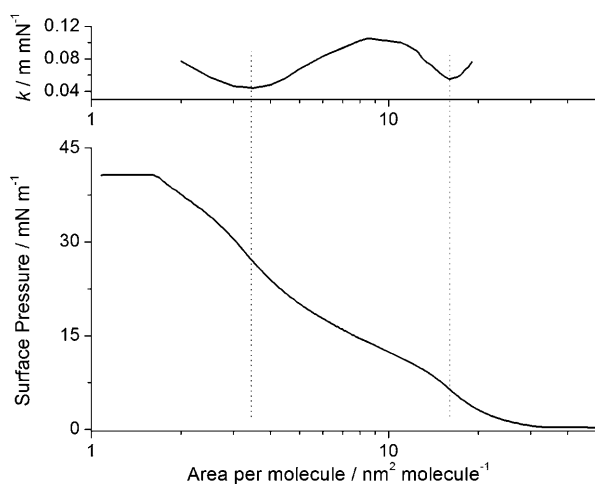


**Figure 1.** Compression isotherm ( $\Pi$ - $A$ ) of PBd-PEO on water and the corresponding surface compressibility  $k = -(1/A)(dA/d\Pi)$ .

ular crowding, a pseudoplateau appears at an area of approximately  $15 \text{ nm}^2 \text{ molecule}^{-1}$ , caused by insertion of PEO segments into the aqueous subphase. The surface pressure of this pseudoplateau ( $\Pi_p = 10 \text{ mN m}^{-1}$ ) agrees well with the plateau of an analogous PEO homopolymer ( $4 \text{ kg mol}^{-1}$ ). However, in contrast to PEO homopolymers, which can be ultimately solubilized into the subphase, the PBd-PEO block copolymer is anchored at the interface by the hydrophobic PBd block. This interfacial anchoring is responsible for the rich two-dimensional phase behavior of polymer monolayers. At still higher surface densities, there is a second transition ( $A < 3.50 \text{ nm}^2 \text{ molecule}^{-1}$ ), which suggests the onset of chain overlap leading to vertical extension, that is, to the formation of a brush. The abrupt flattening of the isotherm at  $\Pi = 41 \text{ mN m}^{-1}$  indicates a collapse, or buckling, of the monolayer.

As is typically reported in the literature,<sup>[8,9,17,18]</sup> the interfacial films herein were only allowed a pause time of 15 min before compression, and therefore such films may be out of equilibrium. Monitoring the pressure over time, after spreading various amounts of material, reveals that equilibrium is not reached until approximately 2–4 h (data not shown). This time dependence is similar to previous adsorption studies that examined the equilibration time of PEO homopolymers at the air/water interface.<sup>[22]</sup> In spite of non-equilibrium conditions, however, the compression isotherm can be reproducibly obtained if the pause time is kept fixed.

### Transferred Monolayer Appears Brushlike in Character

Control over intermolecular conformation and density through compression positioned us to transfer our copolymer films onto hydrophilic substrates (either glass or silicon wafers). Briefly, in the LB method a clean hydrophilic substrate is submerged into the clean water subphase of the trough. Following the application of polymer, a monolayer spontaneously forms with the PEO oriented towards the water and the PBd oriented away from the water. The monolayer is compressed to a desired pressure, and the substrate pulled out vertically

through the interface. As a result of LB deposition, the hydrophilic PEO block preferentially faces towards the substrate while the hydrophobic PBd block preferentially faces away from the substrate. To minimize uncertainty and maintain a uniform film, two clean substrates were fixed “back-to-back” during transfer.<sup>[19,25,26]</sup> As has been recently noted,<sup>[27]</sup> it is important to account for all exposed areas, even the substrate holder, as any surfaces can acquire significant amounts of transferred material.

Figure 2a plots the ellipsometric thickness  $h$  of transferred monolayers as a function of the air/water interfacial density. The interfacial air/water density is simply the inverse of the

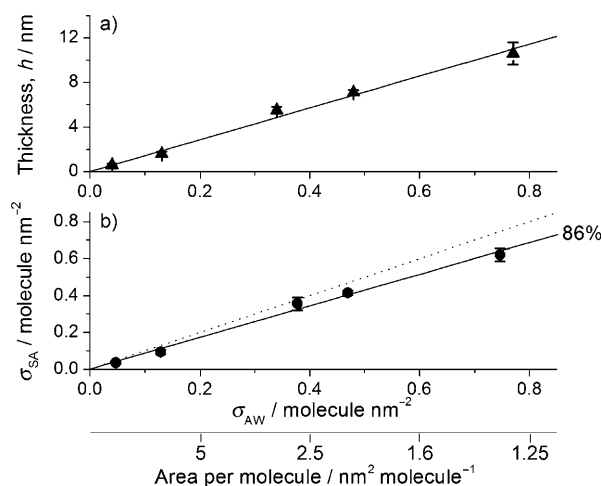


**Figure 2.** a) Transferred film thickness  $h$  as a function of air/water interfacial density  $\sigma_{AW}$  determined by ellipsometry. The linear increase is expected from the conservation of volume. b) “Substrate” interfacial density  $\sigma_{SA}$  as a function of  $\sigma_{AW}$ . The overall transfer efficiency is determined by the best-fit solid line (—), with the perfect transfer represented by the dotted line (.....).

area per molecule,  $\sigma_{AW} = 1/A$ . The increase in thickness with density is linear, as expected from the conservation of volume, and indicates polymer chain extension in the normal direction. De Vos, et al.<sup>[27]</sup> have used  $h$  to estimate “substrate” interfacial densities ( $\sigma_{SA}$ ) of transferred films, by  $\sigma_{SA} = h \cdot \rho$ , where  $\rho$  is the weighed-average bulk density of the block copolymer. The good agreement between experimental and calculated densities (Figure 2b) implies a high efficiency of film transfer by the LB method. The overall efficiency from a best-fit line was found to be 86%, although at the highest interfacial density, the efficiency was slightly lower. For example, the efficiency of deposition at  $\sigma_{AW} = 0.75 \text{ molecule nm}^{-2}$  decreased to 83%. Taken together, a high transfer efficiency and high surface density strongly suggest that this monolayer maintains its brushlike character upon transfer.

The degree of chain stretching in these brushes is expected to be quite strong, because of the very high surface densities achieved by our approach (schematically depicted in Figure 3a). The surface density  $\sigma$  is related to a linear distance  $D$  by the geometrical relation  $\sigma = 4/\pi D^2$ . As noted by de Gennes,<sup>[20]</sup> when  $D$  equals twice the Flory radius ( $R_f$ ), the

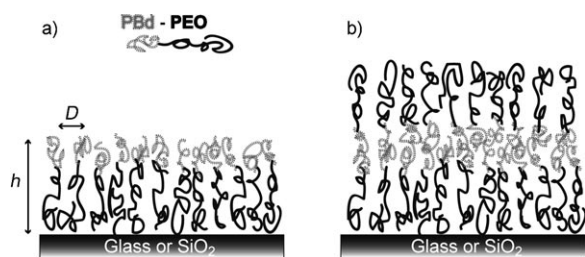


**Figure 3.** a) Idealized schematic of a PBd-PEO brushlike monolayer transferred by the LB method. The film height  $h$  and linear spacing  $D$  are depicted. b) Idealized schematic of a PBd-PEO brushlike bilayer created by a mixed LB/LS technique, which presents a PEO-enriched surface.

chains begin to overlap. Therefore  $D < 2R_F$  is a necessary but insufficient condition for brush formation.<sup>[28]</sup> A “true” brush requires strong vertical chain extension, that is,  $D \ll 2R_F$ . Using typical values for PEO chain dimensions, our formed monolayers and bilayers have  $D/2R_F = 0.10$ . This high chain stretching is key to subsequent surface properties.

The wettability of surfaces (i.e. hydrophilicity/hydrophobicity) can be macroscopically determined by contact-angle measurements. We report both advancing ( $\theta_A$ ) and receding ( $\theta_R$ ) contact angles, because static measurements fail to indicate any hysteresis of the moving water surface. Surfaces with low hysteresis require little energy to displace droplets of liquid. Thus, hysteresis can reveal the presence of heterogeneities due to either surface chemistry or topography that effectively “pin” a moving water droplet, indirectly providing a measure of surface uniformity.<sup>[29]</sup>

With increasing compression (or density) of the copolymer at the interface, the topmost surface of a transferred monolayer should become enriched in the hydrophobic block due to chain extension (Figure 3a). Indeed, the advancing contact angle  $\theta_A$  increases with  $\sigma_{SA}$  indicative of more PBd present at the surface (Figure 4). We presume that the receding angle  $\theta_R$  is significantly lower due to the combination of surface

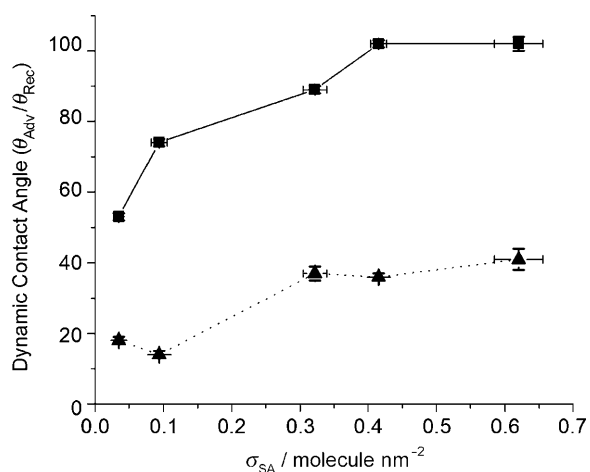


**Figure 4.** Dynamic contact angles of transferred monolayers probed with water. The advancing ( $\blacksquare$ ) and receding contact angles ( $\blacktriangle$ ) both increase with increasing surface density, consistent with a brushlike film. Uptake of water by the underlying PEO is proposed as the cause of hysteresis.

chemistry and any roughness. The probe liquid (water) can diffuse through the PBd to swell the underlying PEO, a process that would be facilitated if the topmost surface is not completely uniform in PBd coverage. In freshly prepared PBd dip-coated surfaces,<sup>[30]</sup> hysteresis is low and a value of  $\theta_A = 108^\circ$  agrees well with our highest-density monolayers (Figure 4). Interestingly, at high densities,  $\theta_R$  approaches the value measured for PEO-grafted silicon surfaces,<sup>[31]</sup> suggesting penetration of the probe liquid (water) into the dried polymer film.<sup>[32]</sup>

### Requirements for Brushlike Bilayer Formation

The high interfacial density of the initial film is crucial to transferring a second monolayer from the interface. At these surface pressures, near the collapse point of the interfacial layer, we have been able to create polymer bilayer films. In the case of PBd-PEO monolayers, the air-exposed PBd blocks must be sufficiently compact or overlapping to provide cohesive interactions. This cohesiveness is needed to minimize any residual stresses in the resulting bilayer, as it has been argued that only at the collapse pressure will the residual stress be identically zero.<sup>[33]</sup> Osborn and colleagues have used this fact to suggest guidelines for efficient bilayer formation, which should be performed close to the collapse pressure.<sup>[34]</sup>

Attempts to sequentially transfer a second monolayer of PBd-PEO by the LB method (vertical deposition starting from the air phase), even at high density, led to detachment of nearly all material upon subsequent vertical removal through the interface. The polymer film originally on the substrate presumably redistributes over the clean air/water interface, although we have not examined if a bilayer is intact before such removal. By contrast, the LS method starts from the air phase and involves horizontally lowering the monolayer substrate through an interfacial layer. Due to a large contact area of favorable hydrophobic-hydrophobic interactions, the LS method successfully transfers a second monolayer. The bilayer nature of these films has been confirmed by a near-doubling of the thickness (Table 1) and agrees well with the predicted value

**Table 1.** Ellipsometric ( $h$ ) and calculated ( $h_{\text{calc}}$ ) thickness of the monolayer and bilayer obtained at a deposition pressure of  $40 \text{ mN m}^{-1}$ .

Surface	$h$ [nm]	$h_{\text{calc}}$ [nm]
Monolayer	$9.9 \pm 0.5$	10.3
Bilayer	$18.1 \pm 1.1$	21.0

calculated by  $h_{\text{calc}} = n^* \sigma_{AW} / \rho$ , where  $n$  is the number of layers. While we refer to these films as bilayers due to their symmetry (Figure 3b), it is likely that there is significant interdigitation of the PBd segments and no clear delineation between the original two monolayers.<sup>[35]</sup> Due to the integer-multiple change in height, and the high surface density ( $D/2R_F \ll 1$ ), successful sequential transfer of a second layer strongly suggests the orientation of the type depicted in Figure 3b. However, surface characterization of dried bilayer films by contact angle is diffi-

cult to interpret due to the inevitable surface reorganization upon drying.<sup>[36,37]</sup> For subsequent experiments, the bilayer was kept from exposure to the interface or air to prevent rearrangement of the film.

### Polymeric Bilayer Resists Protein Adsorption

As opposed to an unstructured film, the topmost surface of our bilayer presents a dense PEO brush (Figure 3b), expected to be resistant to protein adsorption from solution.<sup>[14,38]</sup> By contrast, a monolayer film would present a hydrophobic and attractive interface to proteins.<sup>[39,40]</sup> We therefore determined the ability of our surfaces to resist adhesion by a model protein, fibrinogen. Fibrinogen was chosen because it is found in circulation at a concentration of  $2.6 \text{ mg mL}^{-1}$  and is a key component of the blood-clotting cascade.<sup>[41]</sup>

Following incubation with fibrinogen at  $20^\circ\text{C}$ , changes in thickness of the respective surfaces were measured by ellipsometry.<sup>[14,38,42]</sup> The changes in thickness reveal substantial protein adsorption on monolayer films and significantly less on bilayer films (Figure 5). The relative change in height is even

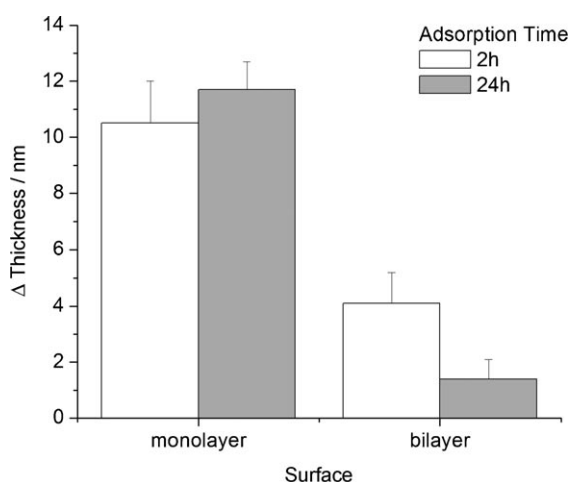


**Figure 5.** Change in thickness of monolayer and bilayer films following incubation with fibrinogen. Enhanced resistance to protein adsorption is found for the hydrophilic bilayer relative to the hydrophobic monolayer.

more pronounced (approx. 100% vs. 10%), since the bilayer is roughly twice as thick as the monolayer. Similar results were obtained when the experiments were carried out at  $37^\circ\text{C}$  (data not shown). Our results are consistent with the tendency of hydrophobic surfaces to adsorb proteins irreversibly, leading to protein unfolding and the displacement of water from the surface.<sup>[41,43,44]</sup> The mechanism for the protein repelling activity of hydrophilic PEO has been argued to be its resistance to release associated water molecules.<sup>[38,42]</sup> The brushlike bilayer sets the stage to provide a relatively bioinert surface for further manipulation.

## Conclusions

By compressing interfacial films of PBd-PEO to nearly the point of collapse, we can achieve dense brushlike conformations. These films can also be efficiently transferred onto solid substrates while maintaining their brushlike character, as confirmed by ellipsometry and wettability. Furthermore, because the bilayer films present PEO at their topmost surface, they have the attractive property of reduced protein adsorption. We expect that such surfaces will be useful to inhibit non-specific cell adhesion. Future work will involve end-labeling our polymers with adhesion ligands such as the tripeptide arginine-glycine-aspartate (RGD), so as to use polymeric bilayer films to control the extent of cell adhesion, spreading, and possibly migration. Importantly, a polymeric brush presents a large fraction of chain ends near the topmost surface, enhancing the presentation of adhesion ligands as compared to other film formulation methods (e.g. LbL, spin-coating). While our cell studies are ongoing, and the subject of another manuscript, preliminary data do suggest reduced cell attachment on native PBd-PEO bilayer surfaces compared to control surfaces.

## Experimental Section

**Materials:** 1,2-Polybutadiene-*b*-poly(ethylene oxide) (6-4k) [PBd<sub>111</sub>-PEO<sub>91</sub>, where the subscripts represent the number of monomeric units] was obtained from Polymer Source, Inc. (Canada) and used as received. Fibrinogen was obtained from Sigma and used as received.

**Dynamic Contact-Angle Measurements:** Contact-angle measurements were conducted with a Ramè-Hart telescopic goniometer equipped with a Gilmont syringe and a 24-gauge flat-tipped needle. Advancing ( $\theta_A$ ) and receding ( $\theta_R$ ) contact angles ( $n=3-5$ ) were determined on the surfaces while the syringe was left in contact with the droplet and used to expand and reduce the size of the drop. The probe fluid was water, purified first by reverse osmosis (RO) followed by Millipore Milli-Q system that involves RO, ion exchange and filtration steps ( $18 \text{ M}\Omega \text{ cm}^{-1}$ )

**Thickness Measurements:** Several measurements ( $n=3-5$ ) of the surface were taken on a Rudolph Ellipsometer Auto EL equipped with a helium-neon laser ( $\lambda=632.8 \text{ nm}$ , angle of incidence  $70^\circ$ ).

**Langmuir Films:** The subphase used was in-house reverse osmosis (RO) water and the air/water interface was aspirated and compressed to remove contaminants. A clean interface was indicated by compression of the interface and resulting a surface pressure remaining below  $0.3 \text{ mN m}^{-1}$ . PBd-PEO was characterized as surface films at the air/water interface. The pressure/area ( $\Pi$ - $A$ ) isotherms were obtained in a Kibron MicrotroughXS (Kibron Inc., Finland). Surface area of trough is  $206 \times 59 \text{ mm}$ . The polymer was dissolved in chloroform:hexane (1:1) ( $50 \mu\text{m}$  filtered) at concentrations of 200, 100, 50, 25 and  $10 \text{ mM}$ . Using a micropipette,  $10-50 \mu\text{L}$  ( $0.1-5.0 \text{ nmol}$ ) were applied dropwise onto the interface. After 15 min to allow for solvent evaporation, the monolayer was compressed by two mobile barriers at a rate of  $591 \text{ mm}^2 \text{ min}^{-1}$ . Our Langmuir balance allows the area to be compressed over one order of magnitude. Therefore, the isotherm was obtained in three overlapping sections to accurately cover the two orders of magnitude range in molecular area.

Langmuir–Blodgett/Langmuir–Schaefer Deposition: The Langmuir monolayer was transferred onto SiO<sub>2</sub> wafers (International Wafer Service, Inc., California, USA) or glass cover slips (diameter 18–22 mm) that had been rinsed with ethanol and RO water and had undergone UV O<sub>2</sub> plasma irradiation (Harrick, 200 millitorr, 10–15 min). For the Langmuir–Blodgett deposition the substrates were aligned perpendicular to the interface and immersed into the subphase before spreading of the polymer solution. After 15 min to allow for solvent evaporation, the monolayer was compressed to the target pressure and held at constant pressure during withdrawal of the substrate at a deposition rate of  $\approx 2 \text{ mm min}^{-1}$ . Once the initial monolayer has dried ( $\approx 2$  hrs), the Langmuir–Schaefer deposition was performed by aligning the surface of the substrate parallel to the clean interface. The polymer solution was spread and after 15 min to allow for solvent evaporation, the monolayer was compressed to the target pressure and held at constant pressure for 5–10 min. The substrate was then allowed to come in contact with the interface for 30–60 s to allow bilayer formation. The interface was aspirated and the barriers relaxed before submerging the bilayer into a collecting beaker in the subphase (and kept underwater for protein adsorption studies). The second monolayer deposition was performed just before protein adsorption studies.

Protein Adsorption Studies: Fibrinogen was dissolved in a phosphate buffer solution (PBS, pH 7.4) at  $1 \text{ mg mL}^{-1}$ . The bilayer in the collecting beaker was moved underwater into a multiwell plate that was in a pan filled with water. The plate was then removed from the pan. Rinsing and exchange of medias were performed to prevent exposure of air to the substrate. Water was aspirated from the wells of the substrate and stopped before the substrate crossed the interface. PBS was gently exchanged three times in this manner. The monolayer was directly placed into empty wells and filled with PBS. The monolayer and bilayer controls were filled with PBS while the test substrates ( $n=2$ ) were gently rinsed and exchanged with the fibrinogen solution three times. Test wells were filled with fibrinogen solution and kept at room temperature for 2 and 24 h. After the incubation time, the substrates were then rinsed and exchanged with water three times and the substrate removed from the well and allowed to dry by blowing N<sub>2</sub> gas gently over the surfaces. After 30 min, the thicknesses ( $n=3-5$ ) of the surfaces were determined by ellipsometry.

## Acknowledgements

This work was financially supported by the NSF Materials Research Science & Engineering Center and by a Healey Endowment Faculty Research Grant. We also thank Micheal Smith for technical assistance.

**Keywords:** amphiphiles · biomembranes · polymers · self-assembly · thin films

- [1] D. J. Irvine, A. M. Mayes, L. G. Griffith, *BioMacromolecules* **2001**, *2*, 85–94.
- [2] G. Decher, *Science* **1997**, *277*, 1232–1237.
- [3] F. Caruso, R. A. Caruso, H. Mohwald, *Science* **1998**, *282*, 1111–1114.
- [4] A. J. Ryan, C. J. Crook, J. R. Howse, P. Topham, R. A. L. Jones, M. Geoghegan, A. J. Parnell, L. Ruiz-Perez, S. J. Martin, A. Cadby, A. Menelle, J. R. P. Webster, A. J. Gleeson, W. Bras, *Faraday Discuss.* **2005**, *128*, 55–74.

- [5] X. W. Fan, L. J. Lin, P. B. Messersmith, *BioMacromolecules* **2006**, *7*, 2443–2448.
- [6] M. Watanabe, Y. Kosaka, K. Sanui, N. Ogata, K. Oguchi, T. Yoden, *Macromolecules* **1987**, *20*, 452–454.
- [7] J. Schneider, H. Ringsdorf, J. F. Rabolt, *Macromolecules* **1989**, *22*, 205–210.
- [8] T. J. Joncheray, K. M. Denoncourt, M. A. R. Meier, U. S. Schubert, R. S. Duran, *Langmuir* **2007**, *23*, 2423–2429.
- [9] R. Matmour, T. J. Joncheray, Y. Gnanou, R. S. Duran, *Langmuir* **2007**, *23*, 649–658.
- [10] K. B. Blodgett, *J. Am. Chem. Soc.* **1935**, *57*, 1007–1022.
- [11] I. Langmuir, V. J. Schaefer, *J. Am. Chem. Soc.* **1938**, *60*, 1351–1360.
- [12] T. Morizumi, *Thin Solid Films* **1988**, *160*, 413–429.
- [13] M. A. Biesalski, A. Knaebel, R. Tu, M. Tirrell, *Biomaterials* **2006**, *27*, 1259–1269.
- [14] H. Du, P. Chandaroy, S. W. Hui, *Biochim. Biophys. Acta. Biomembr.* **1997**, *1326*, 236–248.
- [15] N. V. Efremova, S. R. Sheth, D. E. Leckband, *Langmuir* **2001**, *17*, 7628–7636.
- [16] W. T. E. Bosker, P. A. Iakovlev, W. Norde, M. A. C. Stuart, *J. Colloid Interface Sci.* **2005**, *286*, 496–503.
- [17] R. B. Cheyne, M. G. Moffitt, *Langmuir* **2005**, *21*, 5453–5460.
- [18] A. M. G. da Silva, E. J. M. Filipe, J. M. R. d'Oliveira, J. M. G. Martinho, *Langmuir* **1996**, *12*, 6547–6553.
- [19] J. L. Logan, P. Masse, Y. Gnanou, D. Taton, R. S. Duran, *Langmuir* **2005**, *21*, 7380–7389.
- [20] P. G. de Gennes, *Macromolecules* **1980**, *13*, 1069–1075.
- [21] J. A. Henderson, R. W. Richards, J. Penfold, R. K. Thomas, J. R. Lu, *Macromolecules* **1993**, *26*, 4591–4600.
- [22] J. E. Glass, *J. Phys. Chem.* **1968**, *72*, 4459–4467.
- [23] M. Kawaguchi, M. Tohyama, Y. Mutoh, A. Takahashi, *Langmuir* **1988**, *4*, 407–410.
- [24] L. Deschênes, M. Bousmina, A. M. Ritcey, *Langmuir* **2008**, *24*, 3699–3708.
- [25] E. P. Honig, J. H. T. Hengst, D. Den Engelsen, *J. Colloid Interface Sci.* **1973**, *45*, 92–102.
- [26] C. Scomparin, S. Lecuyer, M. Ferreira, T. Charitat, B. Tinland, *Eur. Phys. J. E* **2009**, *28*, 211–220.
- [27] W. M. de Vos, A. de Keizer, J. M. Kleijn, M. A. C. Stuart, *Langmuir* **2009**, *25*, 4490–4497.
- [28] V. Tsukanova, C. Salesse, *Macromolecules* **2003**, *36*, 7227–7235.
- [29] L. C. Gao, T. J. McCarthy, *Langmuir* **2006**, *22*, 6234–6237.
- [30] K. Baum, J. C. Baum, T. Ho, *J. Am. Chem. Soc.* **1998**, *120*, 2993–2996.
- [31] S. Sharma, R. W. Johnson, T. A. Desai, *Langmuir* **2004**, *20*, 348–356.
- [32] R. V. Sedev, J. G. Petrov, A. W. Neumann, *J. Colloid Interface Sci.* **1996**, *180*, 36–42.
- [33] R. C. Macdonald, S. A. Simon, *Proc. Natl. Acad. Sci. USA* **1987**, *84*, 4089–4093.
- [34] T. D. Osborn, P. Yager, *Biophys. J.* **1995**, *68*, 1364–1373.
- [35] G. Battaglia, A. J. Ryan, *J. Am. Chem. Soc.* **2005**, *127*, 8757–8764.
- [36] S. Ryley, A. T. Chyla, I. R. Peterson, *Thin Solid Films* **2000**, *370*, 294–298.
- [37] Z. Su, D. Wu, S. L. Hsu, T. J. McCarthy, *Macromolecules* **1997**, *30*, 840–845.
- [38] W. R. Gombotz, W. Guanghui, T. A. Horbett, A. S. Hoffman, *J. Biomed. Mater. Res.* **1991**, *25*, 1547–1562.
- [39] A. S. Hoffman, *J. Biomed. Mater. Res.* **1986**, *20*, R9–R11.
- [40] T. A. Horbett, J. L. Brash, *ACS Symp. Ser.* **1987**, *343*, 1–33.
- [41] P. Roach, D. Farrar, C. C. Perry, *J. Am. Chem. Soc.* **2005**, *127*, 8168–8173.
- [42] K. L. Prime, G. M. Whitesides, *J. Am. Chem. Soc.* **1993**, *115*, 10714–10721.
- [43] J. J. Gray, *Curr. Biol. Curr. Opin. Struct. Biol.* **2004**, *14*, 110–115.
- [44] B. D. Ratner, S. J. Bryant, *Annu. Rev. Biomed. Eng.* **2004**, *6*, 41–75.

Received: September 18, 2009

Revised: November 4, 2009

Published online on December 22, 2009